

Time-series analysis of phase dynamics in a campus distribution grid using short-term Koopman mode decomposition

Munetaka Noguchi[†], Yoshihiko Susuki[‡], and Atsushi Ishigame^{††}

[†]Department of Electrical and Information Systems, Osaka Prefecture University
 1-1 Gakuen-cho, Naka-ku, Sakai 599-8531, Japan

[‡]Department of Electrical Engineering, Kyoto University
 Katsura, Nishikyo-ku, Kyoto 615-8510, Japan

^{††}Department of Electrical and Electronic Systems Engineering, Osaka Metropolitan University
 1-1 Gakuen-cho, Naka-ku, Sakai 599-8531, Japan

Email: sbb01137@st.osakafu-u.ac.jp, susuki.yoshihiko.5c@kyoto-u.ac.jp, ishigame@omu.ac.jp

Abstract—Recently, the so-called micro-Phasor Measurement Unit (PMU) with high-resolution capability has been expected as a new data-driven technology of analysis and control of the future power distribution system. In this report, we analyze non-stationary time-series data on voltage-phase differences derived by multiple micro-PMUs for the campus distribution network in Osaka Metropolitan University, Japan. The analysis is based on a short-term Koopman mode decomposition that is based on eigenvalues of the Koopman operator for a nonlinear time-variant system (as a latent model of dynamics of the distribution system). We visualize that dominant Koopman modes and associated frequencies embedded in the time-series change as time goes on.

1. Introduction

The utilization of Phasor Measurement Units (PMUs) in power distribution systems has been recently investigated (see, e.g., [1]). This is because state monitoring and operation of power distribution systems are expected to become more complicated due to the high penetration of renewable energy sources and electric vehicles. The so-called micro-PMU (μ PMU) is capable of measuring the phase difference of AC voltage at multiple points in a distribution system and deriving time-stamped data on the phase difference with high accuracy [2, 3].

We reported our project on real-field measurement and data analysis for the campus distribution network in Nakamozu campus, Osaka Metropolitan University, Japan [4, 5]. In the measurement, the four μ PMUs are placed in the low-voltage distribution system in order for us to collect data on the amplitude, frequency, and phase of three-phase AC voltage [4]. In the data analysis, we use the so-called Koopman Mode Decomposition (KMD) [6], which is based on Koopman operator theory of nonlinear dynamical systems [7]. KMD is a novel method for decomposing time-series data representing complex dynamics into

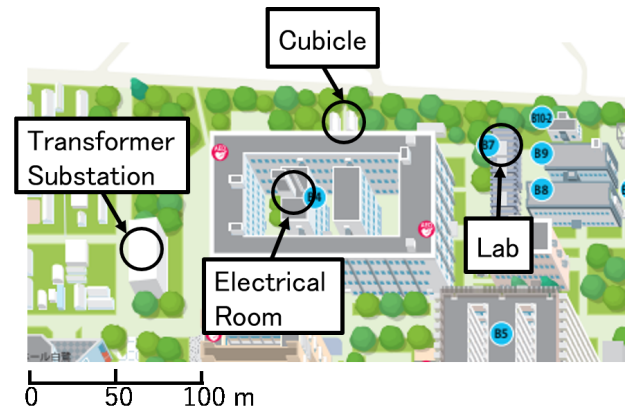





Fig. 1: Four measurement locations of μ PMUs for measurement of distribution grid in Nakamozu campus, Osaka Metropolitan University, Japan

modes with a single frequency (called Koopman modes).

The purpose of this report, following [4, 5], is to introduce a data analysis for non-stationary dynamics of phase differences for the campus distribution grid in terms of KMD. Generally speaking, distribution systems are directly affected by load variations compared to wide-area transmission systems because the electrical distance between distribution system and load is very short. Because such load variations are typically non-periodic, it becomes natural to explicitly consider time-variant characteristics in the KMD. Koopman operators for time-variant dynamical systems are discussed in [8], and the Dynamic Mode Decomposition (DMD [9]; as a numerical algorithm of KMD) for actuated dynamics are also discussed in [10, 11, 12]. In this report, we show time-series data of the voltage-phase differences derived by the four μ PMUs in Sect. 2. Then, we introduce an idea of short-term KMD for nonlinear time-variant systems based on [8] in Sect. 3 and apply it to the time-series data of Sect. 2. Conclusions of this report are presented in Sect. 4. Note that a preliminary version of this report is in non-reviewed conference proceeding [13]

ORCID iDs First Author:  0000-0002-2400-9793, Second Author:
 0000-0003-4701-1199, Third Author:  0000-0002-8470-5774



This work is licensed under a Creative Commons Attribution NonCommercial, No Derivatives 4.0 License.

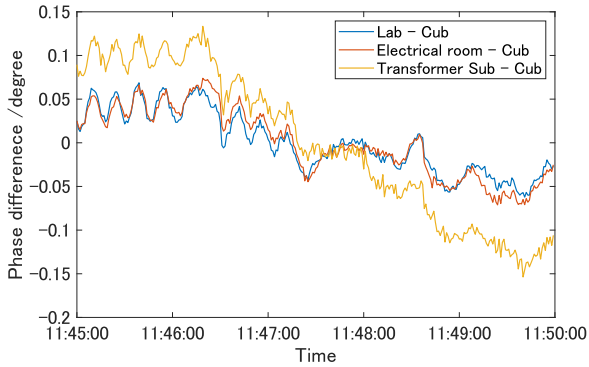


Fig. 2: Time-series data of voltage-phase differences on October 7, 2020 in JST

in Japan.

2. μ PMU data

Figure 1 shows an overview of measurement of the campus distribution grid in Nakamozu campus of Osaka Metropolitan University, Japan. The four μ PMUs are connected to 3-phase 220 V terminals at four places (Lab, Electrical room, Cubicle, and Transformer Substation). At the four locations, time-stamped data on AC voltage amplitude, frequency, and phase angle are derived and sent to a local data server. In this report, we focus on the difference of voltage-phases for our data analysis. Fig. 2 shows time-series data of the three phase differences during five minutes starting from 11:45 on October 7, 2020 in JST. The horizontal axis of the figure is the time, and the vertical axis is the three phase differences with respect to Cubicle: Lab, Electrical room, and Transformer Sub. Note that to plot the data, all the time-averaged components were removed. The sampling interval is one second. In the time-series data, excitations of multiple frequency components and their time variations, which might be due to load changes, are observed.

3. Method and data analysis

3.1. Koopman operator for time-variant systems

First, we introduce a Koopman operator for time-variant systems. For this, we consider the following nonlinear time-variant dynamical system evolving in n -dimensional Euclidean space \mathbb{R}^n :

$$\dot{\mathbf{x}} = \mathbf{F}(\mathbf{x}, t), \quad \mathbf{x} \in \mathbb{R}^n, t \in \mathbb{R}, \quad (1)$$

where \mathbf{x} is the state variable and t is the continuous time. \mathbf{F} is a nonlinear vector field, which corresponds to a latent dynamical model (but unknown) for the target campus distribution grid in this report. We denote the solution of the above equation passing through state \mathbf{x}_0 at initial time t_0 by

$\varphi^{(t,t_0)}(\mathbf{x}_0)$ ($t \geq t_0$) (clearly, $\varphi^{(t_0,t_0)}(\mathbf{x}_0) = \mathbf{x}_0$). In addition, we denote the scalar-valued function defined on the state space \mathbb{R}^n by f , which we call the observable. The linear space consisting of all the observables is denoted by \mathcal{F} . By using these notations, the Koopman operator for the time-variant system (1) is introduced as the following composition [8]:

$$U^{(t_0,t)} f := f \circ \varphi^{(t,t_0)}, \quad f \in \mathcal{F}. \quad (2)$$

This $U^{(t_0,t)} : \mathcal{F} \rightarrow \mathcal{F}$ is a linear operator that possesses the two parameters related to time, t, t_0 ($t \geq t_0$). In addition, $U^{(t_0,t_0)}$ is the identity operator on \mathcal{F} and satisfies the so-called co-cycle property $U^{(t_0,t_2)} = U^{(t_0,t_1)} U^{(t_1,t_2)}$ for $t_2 \geq t_1 \geq t_0$.

The eigenvalue of the Koopman operator $U^{(t,t_0)}$ is discussed in [8]. The Koopman eigenvalue, denoted by $\mu(t_0, t)$, possesses the two parameters t, t_0 . The $\mu(t_0, t)$ and associated Koopman eigenfunction $\phi_{\mu(t_0,t)}$ are formally introduced as follows:

$$U^{(t_0,t)} \phi_{\mu(t_0,t)} = e^{\mu(t_0,t)} \phi_{\mu(t_0,t)}, \quad \phi_{\mu(t_0,t)} \neq 0. \quad (3)$$

If (1) is a linear system, then an analytical treatment of Eq. (3) based on the fundamental solution matrix is given in [8].

3.2. Short-term Koopman mode decomposition

In this report, we will approximate Eq. (3) in a similar manner as [14]. For this, let $h = t - t_0$ be a small positive constant and let us assume that the eigenvalue $\mu(t_0, t_0 + h)$ can be expanded with respect to h like

$$\mu(t_0, t_0 + h) = \lambda^{(t_0)} h + \text{h.o.t.}, \quad (4)$$

where $\lambda^{(t_0)}$ is the expansion coefficient of the first-order term, and the high-order term (h.o.t.) includes at least h^2 . The operator $U^{(t_0,t_0)}$ is the identity, hence the term independent of h does not appear on the right-hand side of Eq. (4). Now, from Eqs. (3) and (4), we introduce the following approximation of Eq. (3) as

$$U^{(t_0,t_0+h)} \phi_{\lambda^{(t_0)}} = e^{\lambda^{(t_0)} h} \phi_{\lambda^{(t_0)}}, \quad h \geq 0, \quad (5)$$

where $\phi_{\lambda^{(t_0)}}$ can be introduced in the same manner as $\lambda^{(t_0)}$ through the expansion. It is supposed that there exists a positive h^* such that this approximation is held for all $h \in [0, h^*]$. By regarding the initial time t_0 as a parameter, Eq. (5) is almost the same as the definition of Koopman eigenvalue and eigenfunction for time-invariant systems [15]. Then, by choosing T from $(0, h^*)$ and using sampled data of $\mathbf{x}(t)$ in the finite interval $[t_0, t_0 + T]$ while shifting t_0 in forward time, it is possible to estimate approximations of $\lambda^{(t_0)}$ and associated modes by DMD algorithms, where in this paper we use the Arnoldi-type algorithm [6]. We term the present analysis as *Short-Term Koopman Mode Decomposition* (STKMD).

Here, following the method in Short-Term Fourier Transform (STFT) [16], we use the so-called window function $w(t)$ for the recursive computation of the Koopman eigenvalues. There are many window functions used in signal processing (see [17]). By using $w(t)$, our target is the sampled data of $\mathbf{x}_T(t)$ in $[t_0, t_0 + T]$ defined as

$$\mathbf{x}_T(t) = w(t - t_0)\mathbf{x}(t). \quad (6)$$

It should be noted that STKMD is similar to STFT. One difference is that STKMD is capable of estimating damped oscillatory dynamics as point spectra, while STFT as continuous spectra. Another is that STKMD can take a variable resolution in the frequency domain, while STFT does a fixed one.

3.3. Result

Table 1 shows the STKMD for the time-series data on voltage-phase differences in Fig. 2 by different window sizes T and window functions $w(t)$. We set the window size $T/s = 32, 64, 128$ and the initial time $t_0/s = 0, 1, \dots, 300 - T$ for the finite interval $[t_0, t_0 + T]$. Also, the three window functions from [17]—Hamming window, Hanning window, and Blackman window—are used, then the frequencies determined from the Koopman eigenvalues and Koopman modes for the finite interval are computed. The sampling period for the analysis corresponds to that in Fig. 2: one second. The horizontal axis for each figure in Tab. 1 shows the frequency, and the vertical axis shows the initial time t_0 . We can see that the points are plotted at different intervals in the frequency axis, which is one of the advantages of STKMD. In each of the figures, by using the color (red), we show the vector norm of Koopman modes obtained in each interval. The largest vector norm of the Koopman modes is set as the reference value. A computed Koopman mode which vector norm is close to the reference value is plotted in darker color. Therefore, the dark-colored points in the figures represent dominant Koopman modes for the time-series data.

Now, we discuss the dependence of the choice of window size and window function. By comparison with the Hanning and Blackman windows, the results with the Hamming window clearly visualize that the distribution of dominant Koopman modes changes as time goes on. Here, we can see that the distribution of dark-colored points around 0.05 Hz is consistent with the initial time. These dominant modes contain the frequency component corresponding to the oscillation with a period of about 20 seconds, which is regularly excited in Fig. 2. Also, we see that as T increases, the frequency resolution increases, i.e., the distribution of Koopman modes becomes dense in terms of the horizontal axis. In the case of using the Hanning and Blackman windows, the dark-colored points are mostly localized at 0 Hz and 0.5 Hz, and temporal changes of dominant Koopman modes are not clear by comparison with the case of using the Hamming window. These suggest that the STKMD

computation depends on the choice of window size and window function. Its criterion in terms of time-series analysis is not clarified and remains unsolved.

4. Conclusion

In this report, we showed the result of short-term KMD by three different window sizes and window functions (Hamming window, Hanning window, and Blackman window) applied to the measurement data of voltage-phase differences collected by μ PMU in the campus distribution grid. The short-term KMD was introduced from the Koopman operator for time-variant systems. We visualized that the distribution of dominant Koopman modes change as time goes on in the case of using the Hamming window.

Several open problems exist. One is to consider how the window size T affects the temporal resolution of the short-term KMD. Another is to compare the proposed spectral computation with existing different ones.

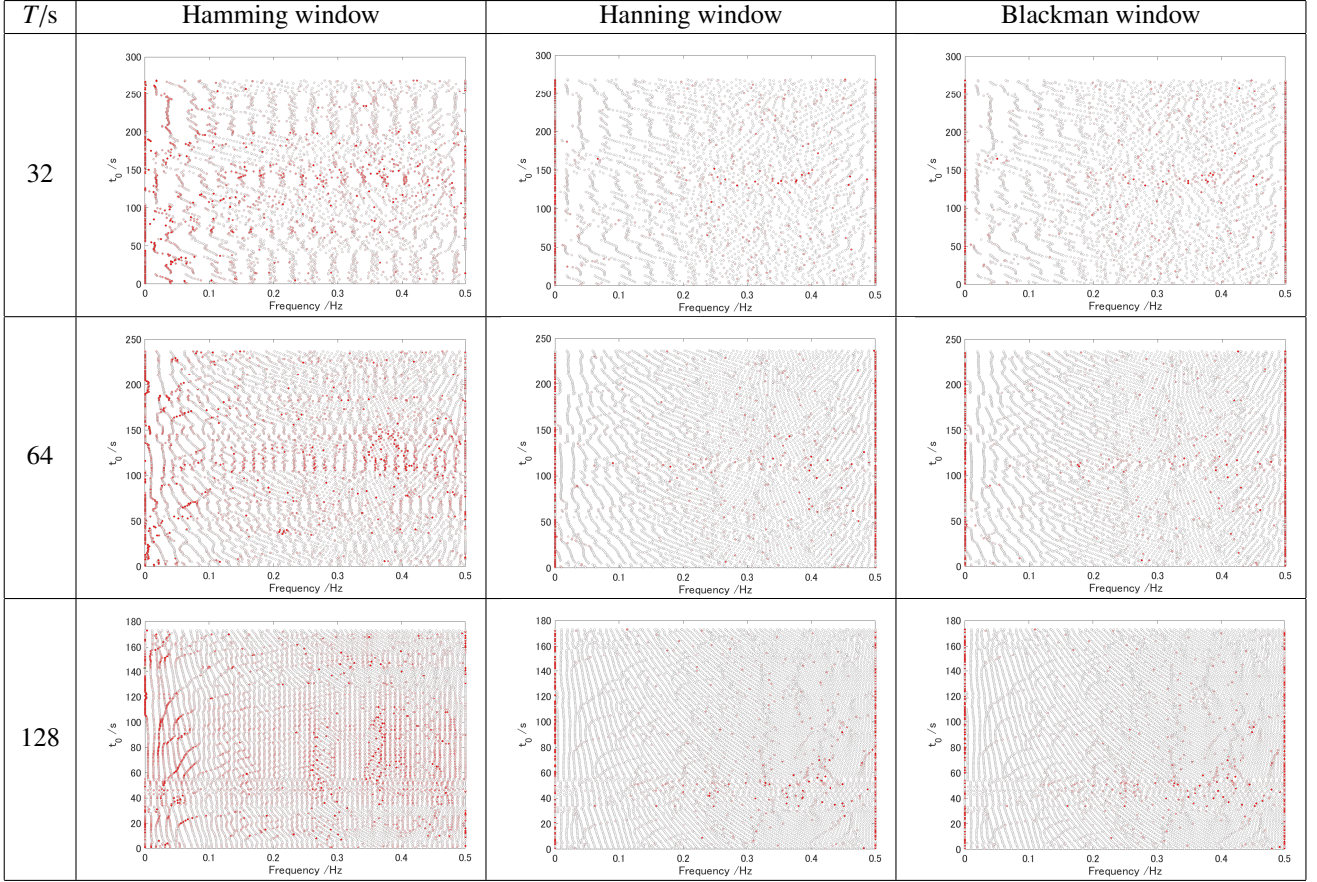
Acknowledgment

This work was supported in part by JST PRESTO (JP-MJPR1926).

References

- [1] Muhammad Usama Usman and M Omar Faruque. Applications of synchrophasor technologies in power systems. *Journal of Modern Power Systems and Clean Energy*, 7(2):211–226, 2019.
- [2] Reza Arghandeh. Micro-synchrophasors for power distribution monitoring, a technology review. *Preprint arXiv:1605.02813*, 2016.
- [3] Alexandra Von Meier, Emma Stewart, Alex McEachern, Michael Andersen, and Laura Mehrmanesh. Precision micro-synchrophasors for distribution systems: A summary of applications. *IEEE Transactions on Smart Grid*, 8(6):2926–2936, 2017.
- [4] Munetaka Noguchi, Yoshihiko Susuki, Takahiro Shimomura, and Atsushi Ishigame. A study on synchronized phasor measurement data in campus distribution grid. In *Proceedings of the Symposium of SICE Kansai Branch & ISCIE*, B3-3, 2020. (in Japanese).
- [5] Munetaka Noguchi, Yoshihiko Susuki, and Atsushi Ishigame. A study on prediction of synchrophasor time-series data of in-campus distribution voltage using gaussian process regression. In *Technical Reports of IEICE*, volume 121, pages 10–13, 2021. (in Japanese).
- [6] Clarence W Rowley, Igor Mezić, Shervin Bagheri, Philipp Schlatter, and Dans Henningson. Spectral analysis of nonlinear flows. *Journal of Fluid Mechanics*, 641(1):115–127, 2009.

Table. 1: STKMD applied to the time-series data in Fig. 2 with different window sizes and window functions



- [7] Alexandre Mauroy, Yoshihiko Susuki, and I Mezić. *The Koopman Operator in Systems and Control*. Springer Nature, 2020.
- [8] Senka Maćešić, Nelida Črnjarić-Žic, and Igor Mezić. Koopman operator family spectrum for nonautonomous systems. *SIAM Journal on Applied Dynamical Systems*, 17(4):2478–2515, 2018.
- [9] J Nathan Kutz, Steven L Brunton, Bingni W Brunton, and Joshua L Proctor. *Dynamic Mode Decomposition: Data-Driven Modeling of Complex Systems*. SIAM, 2016.
- [10] Matthew O Williams, Maziar S Hemati, Scott TM Dawson, Ioannis G Kevrekidis, and Clarence W Rowley. Extending data-driven Koopman analysis to actuated systems. *IFAC-PapersOnLine*, 49(18):704–709, 2016.
- [11] Hao Zhang, Clarence W Rowley, Eric A Deem, and Louis N Cattafesta. Online dynamic mode decomposition for time-varying systems. *SIAM Journal on Applied Dynamical Systems*, 18(3):1586–1609, 2019.
- [12] Joshua L Proctor, Steven L Brunton, and J Nathan Kutz. Dynamic mode decomposition with control. *SIAM Journal on Applied Dynamical Systems*, 15(1):142–161, 2016.
- [13] Munetaka Noguchi, Yoshihiko Susuki, and Atsushi Ishigame. A study on dynamic characteristics of voltage-phase differences in a campus distribution using Koopman mode decomposition. In *Proceedings of the 66th Annual Conference of the Institute of Systems, Control and Information Engineers (ISCIE)*, number 212–5, pages 452–455, 2022. (in Japanese).
- [14] Alexandre Mauroy, Yoshihiko Susuki, and I Mezić. Introduction to the Koopman operator in dynamical systems and control theory. In *The Koopman Operator in Systems and Control*, chapter 1. Springer Nature, 2020.
- [15] Igor Mezić. Analysis of fluid flows via spectral properties of the Koopman operator. *Annual Review of Fluid Mechanics*, 45:357–378, 2013.
- [16] Daniel Griffin and Jae Lim. Signal estimation from modified short-time fourier transform. *IEEE Transactions on Acoustics, Speech, and Signal Processing*, 32(2):236–243, 1984.
- [17] John G Proakis and Dimitris G Manolakis. Design of digital filters. In *Digital Signal Processing: Principles, Algorithms, and Applications*, chapter 8. Prentice-Hall, Inc., 1996.